投稿論文(英文)
PAPERS

J. Geotech. Eng. No. 481/III—25, pp. 175~186, December 1993

DISLOCATION ENERGY OF LIQUEFACTION

Shunichi IGARASHI*

The relation between the total kinematic energy and dislocation energy of soil in pore-water is derived from a physical premise and the conservation law of the multiphase-continuum, assuming that the internal friction of soil is idealized by the sliding block model. A pair of material constants are identified to characterize the strength of soil against liquefaction. The procedure to measure them from the cyclic undrained test data is developed. This method is applyed to the liquefaction observed in the Kawagishi-cho during the 1964 Niigata earthquake.

Key Words: *liquefaction, undrained testing, dislocation, energy, ground motion*

1. INTRODUCTION

Soil consists of many particles and void. The void is filled with fluid and gas. The three components move, interacting with each other, in response to the action of external forces. A part of the mechanical properties of soil has been explained by the theory of elasticity (Biot, 1956; Ishihara, 1968). Yet, the actual deformation of soil differs considerably from what the elasticity theory predicts as the magnitude of loading increases. The accumulation of pore-water pressure and eventual liquefaction is a result of this inelastic or plastic deformation of soil. Thus, the description of the plasticity of soil is essential in analyzing liquefaction.

The plasticity of solid is attributed to the line defects of crystals, called dislocations (Myers, 1990). This concept was introduced by Taylor in 1934, in an attempt to explain that the actual metal is much softer than it is predicted by assuming that the crystal has no defect (Suzuki, 1989). The first direct experimental evidence for their existence came in 1948. A dislocation stores energy in the elastic strain field surrounding it when it moves. The ratio between the stored energy and the dissipated energy, through plastic deformation or motion of dislocation, is found theoretically to be $\pi/21=0.15$(Cocks and Ponter,1991) and experimentally to be about 10 to 15% (Titchener & Beven, 1958). Both experimentally and theoretically, the mechanical property of metal is explained by the microscopic structure.

The particles of the soil are by far more randomly arranged in comparison to those of metal, which are almost periodic. Therefore, the microscopic modeling of soil should take this randomness into account in order to explain the mechanical property of soil. Also, the ground motion due to earthquakes is random. Liquefaction requires statistical treatment in both the loading and material categories. However, for a small increment of time and space, the author fields that the plastic deformation of soil can be regarded as localized in a certain structure of particles which we call the dislocation of soil.

When saturated soil, with negative dilatancy or contractancy, is sheared, the pore-water is drained. If the same soil is sheared and the drainage of the pore-water is prevented, we observe an increase of the pore-water pressure, i.e. its strain energy. The plastic deformation of soil also accompanies strain energy storage. We call this energy the dislocation energy of soil in pore-water. In this paper, we attempt to construct a theoretical framework to explain liquefaction.

2. ENERGY IN THE SOIL

Consider a bulk of soil that occupies a finite volume in space and time. Some work W, done on the bulk of soil, changes the soil's kinematic energy K, potential energy due to the gravity H. The other part of the external work W is either stored as internal energy E or dissipated through internal friction D:

$$W=\Delta E+\Delta K+\Delta H+D \cdots\cdots\cdots\cdots\cdots\cdots (1)$$

We assume that the bulk of soil is composed of a skeleton and pore-material:

*Member of JSCE, Dr. Eng. Taisei Corporation, Tokyo, Japan

$$E=E_s+E_p \quad \cdots\cdots (2)$$

where subscript s and p denotes the skeleton and pore, respectively. We assume that the pore is filled with water and that the water is homogeneous linear elastic material without shear rigidity. The strain energy density of the pore-water is written in terms of the pressure p:

$$E_p = \frac{1}{2} n_f C p^2 \quad \cdots\cdots (3)$$

where n_f and C is the porosity and compressibility, respectively. Then, the change in pore-pressure is related to the change in the strain energy:

$$\Delta p = p - p_0 = \sqrt{\frac{2\Delta E_p}{n_f C} + p_0^2} - p_0 \quad \cdots\cdots (4)$$

3. DISLOCATION ENERGY IN THE PORE-WATER

Soil can transport external work in the form of elastic waves as a periodic exchange of kinematic and elastic energy. We assumed, writing Eq. (1), that a part of the energy is dissipated through the internal friction. In some types of soil, we observe the residual increment in the pore-water pressure as well as the plastic deformation. This means that a part of the external work is stored in the pore-water as its strain energy. In other words, the plastic deformation of soil accompanies a permanent increment of the strain energy in the pore-water. We call this energy the dislocation energy in the pore-water:

$$\Delta E_{ps} = \eta D \quad \cdots\cdots (5)$$

where the subscript s denotes that ΔE_{ps} is the permanent increment of ΔEp, D is the energy dissipated through internal friction, and η is a non-dimensional factor that we call the energy absorption ratio of pore-water. This factor represents both the permanent volumetric change in the structure of the soil associated with the internal friction and the local drainage condition. If the soil deforms plastically without changing volume, then $\eta=0$. If it dilates, $\eta<0$. If the soil contracts during plastic deformation and the drainage is prevented, then $\eta>0$. Generally, this factor is a function of both material property of soil and characteristics of loading. In constructing our theory of liquefaction, we will assume that η is constant for sand with small to medium density.

4. SLIDING BLOCK MODEL OF INTERNAL FRICTION

In Eqs. (1) through (5), we quantifyed, by introducing a ratio η, that the plastic deformation of soil associates the energy dissipation as well as the energy storage in the pore-water. The remaining element of our model is the description of the energy dissipation mechanism. We assume, at least for a small increment of time, that the plastic deformation of soil is localized in a certain structure called the dislocation of soil as illustrated in **Fig. 1 (a)**. Some particles are located linearly to form a potential sliding surface for the hatched particles. When the load on these particles exceeds the frictional resistance along the sliding surface, they start to slide. If we neglect the elastic deformation and the relative motion within the hatched particles, then they are represented by the block on the rough boundary in **Fig. 1 (c)**. This simplification is the same as introduced by Newmark to analyze the permanent deformation of rock-fill dams. During sliding, the hatched particles receive resistance from other particles, and pore-water as illustrated in **Fig. 1 (b)**. We assume the reaction from the pore-water is small compared with the friction, in other words, the ratio η in Eq. (5) is by far smaller than unity. Then the internal force of the sliding block model becomes only friction between the block and the rough plane which, we assume, is of the Coulomb type with the friction angle ϕ. Finally, this model is determined by a pair of angles ϕ and α, the latter being the inclination of the plane from the horizontal. These parameters are compressed into one by defining the critical acceleration against sliding (Igarashi and Hakuno, 1987):

$$A_c = G\sin(\phi-\alpha) \quad \cdots\cdots (6)$$

which is the minimum magnitude of the absolute acceleration of the block that initiates sliding, and where G is the gravity constant.

The response of this model, due to random excitations, was investigated and an analytical expression of the mean slip displacement S was obtained as a function of the parameters which characterize the absolute acceleration of the rough plane (Igarashi and Hakuno, 1987).

$$S=\frac{s_0 a_{rms}^2}{2\pi\omega_a A_c}\exp\left(-\frac{1}{2}\left(\frac{A_c}{a_{rms}}\right)^2\right)\left(1+\frac{\pi}{2}\frac{\sqrt{1-\alpha_v^2}}{\alpha_v}\right) \cdots (7)$$

where, a_{rms} and ω_a is the Root Mean Square amplitude and the central frequency of the acceleration of the rough plane. α_v is the bandwidth parameter of its velocity which is theoretically bounded between zero and unity corresponding to white noise and a sinusoid. s_0 denotes the strong motion duration of Vanmarcke and Lai's definition (1980). They are determined from the power spectral density function of the input motion.

By multiplying both sides of Eq. (7) with $2\rho A_c$, ρ as the density of the mass and the rough plane, and rearranging the terms, noting the definition of the bandwidth parameter α_v and RMS velocity v_{rms}:

$$\alpha_v=\frac{\omega_v}{\omega_a},\ v_{rms}=\frac{a_{rms}}{\omega_v} \cdots\cdots (8)$$

where ω_v is the central frequency of velocity. Then the energy dissipated through friction D is related to a quantity which we call the total kinematic energy density of the input motion:

$$\bar{K}N_v=\frac{s_0\rho v_{rms}^2\omega_v}{2\pi} \cdots\cdots (9)$$

i.e., Eq. (7) is written as

$$D=2\rho A_c S=2f\bar{K}N_v \cdots\cdots (10)$$

$$f=\exp\left(-\frac{1}{2}\left(\frac{A_c}{a_{rms}}\right)^2\right)\left(\alpha_v+\frac{\pi}{2}\sqrt{1-\alpha_v^2}\right) \cdots (11)$$

where ρA_c represents the mean force acting between the unit mass and rough plane. The factor 2 is introduced to account for the fact that the mass can move to both sides since the original analytical expression is obtained by assuming the motion is one-sided. $\bar{K}$ is the mean kinematic energy:

$$\bar{K}=\frac{1}{2}\rho v_{rms}^2 \cdots\cdots (12)$$

And

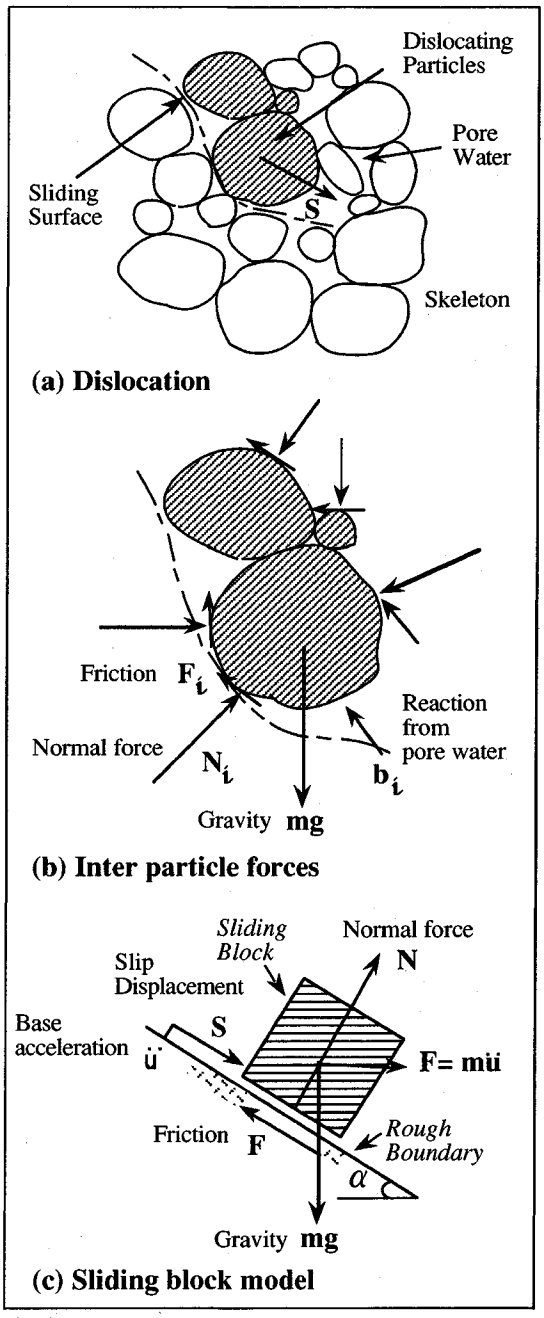

Fig. 1 Sliding block model for internal friction of soil

$$N_v=\frac{s_0\omega_v}{\pi} \cdots\cdots (13)$$

is the mean number of cycles of the energy or velocity squared.

The function f in Eq. (11) relates the mean kinematic energy with the energy loss in one cycle of loading. The last component of Eq. (11) just scales its

magnitude between 1 and $\pi/2=1.578$ when α_v varies from zero to unity taking its maximum of $\sqrt{\pi^2+4}/2=1.862$ at $\alpha_v=2/\sqrt{\pi^2+4}=0.537$. The first component starts from unity and decays exponentially as the critical acceleration increases. We will show that this function f is related to the damping coefficient in the next chapter.

A unit volume of soil is expected to possess a number of dislocations with various orientations and lengths. During a finite time, dislocations may slide many times and new slip surfaces or dislocations may be created. We assume that for each dislocation and slip event, the above formulae apply. Therefore, if we sum up all the energy dissipated in a finite volume of soil and then compare it with the mean kinematic energy, a relation in the form of Eq. (10) can be obtained and Eq. (11) will define, implicitly, a critical acceleration of a unit volume of soil. If the soil is granular or the inter particle force is Coulomb friction, then the resistance against sliding is proportional to the normal force with friction angle ϕ. But the normal force can vary from dislocation to dislocation and can change during the loading. We will use the initial effective confining stress σ_{m0}' to represent the magnitude of the normal forces of local slip surfaces in a unit volume. And assume that critical acceleration of a unit volume of soil is written:

$$A_c=\frac{\sigma_{m0}'}{\rho l}\tan\phi_c \cdots\cdots\cdots\cdots\cdots\cdots (14)$$

where ρ is the mass density of the bulk. A coefficient l with the dimension of length is introduced, which is determined from the relationship between the shear stress and the acceleration of the unit volume of soil. If the soil is layered horizontally receiving a lateral uniform acceleration, then the factor l is the depth H from the ground surface.

From Eqs. (5) and (10), the energy stored in the pore-water due to generic random excitation is obtained:

$$\Delta E_{ps}=2\eta f \bar{K} N_v \cdots\cdots\cdots\cdots\cdots\cdots (15)$$

5. MEASUREMENT OF THE MATERIAL PARAMETERS

Our model brought forth three new material constants relevant to liquefaction, namely the compressibility of the pore-water C (Pa^{-1}), the energy absorption ratio η and the critical angle of dislocation ϕ_c. These constants are defined so generally that, to measure the parameters, it is not necessary to develop special devices but rather to just solve the equation under the conditions of the existing test procedure. Although the resolution depends on the type of test and field measurement, if the model and hypotheses conform to the reality, they can be evaluated during various occasions when liquefaction occurs. This is an advantage of our formulation compared to the conventional indices defined in a specific environment.

The resistance of soil against liquefaction has been measured in the undrained cyclic shearing test either by triaxial or torsional loading; the standard method of the former has been specified by the Japanese Society of Soil Mechanics and Foundation Engineering(Toki et.al, 1986). In either case, the test results are expressed in the form of the R_l vs. N chart; the cyclic stress ratio that cause 5% or 10% double amplitude of axial strain are plotted against the number of cycles required. In the following we will see just how the material constants are determined by the test data.

Consider a small volume of soil inside the specimen used for cyclic undrained testing. We analyze the liquefaction in this specimen using the Cartesian coordinate system xyz, and time t. The z axis is in the direction of the gravity; the origin is at the center of the top surface of the specimen. Assume the soil is uniform in the xy directions. The equation of motion for the differential volume of the soil with shear rigidity G and mass density ρ yields the one-dimensional wave equation.

$$\frac{\partial\tau}{\partial z}=G\frac{\partial^2 u}{\partial z^2}=\rho\frac{d^2u}{dt^2} \cdots\cdots\cdots\cdots\cdots (16)$$

where τ and u are the magnitude of the shear stress and displacement on the plane normal to the z axis.

Suppose that, at rest, the soil is in such a stress state with three effective principal stresses being σ_{v0}', $K_0\sigma_{v0}'$, and $K_0\sigma_{v0}'$. Either by controlling the vertical stress or by applying the shear stress directly, the soil is supposed to suffer cyclic shear stress of amplitude τ_d.

$$\tau=\tau_d\sin\omega t \cdots\cdots\cdots\cdots\cdots\cdots (17)$$

in which ω is the angular frequency. The mean strain energy in the specimen per unit period of loading $T_0=2\pi/\omega$ is calculated from Eq. (17)

$$\bar{E}=\frac{1}{T_0}\int_0^{T_0}\frac{\tau_d^2}{2G}\sin^2\omega t\,dt\equiv\frac{\tau_{rms}^2}{2G}=\frac{\tau_d^2}{4G} \cdots (18)$$

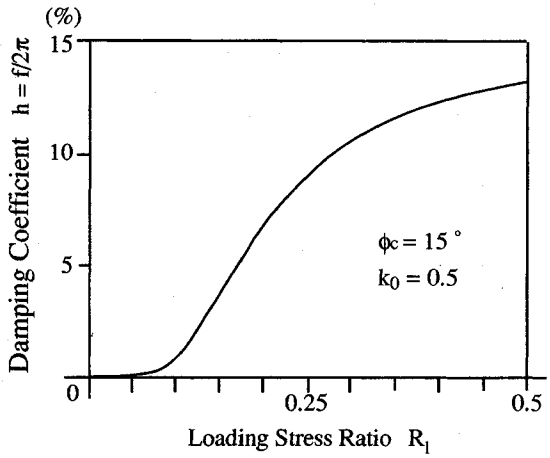

Fig.2 Damping Coefficient of Sliding Block Model

where τ_{rms} stands for the Root Mean Square amplitude of the shear stress τ.

The effect of the external loading is assumed to propagate through the specimen as the elastic wave described in Eq. (16). Therefore, the mean kinematic energy is equal to the mean strain energy:

$$\frac{1}{2}\rho v_{rms}^2 = \frac{1}{2}G\gamma_{rms}^2 = \frac{\tau_{rms}^2}{2G} \quad \cdots\cdots\cdots (19)$$

where $\gamma_{rms} \equiv (\partial u/\partial z)_{rms}$ is the Root Mean Square amplitude of shear strain. From Eqs. (18) and (19), and noting the relationship $G=\rho\omega^2/k^2$, the RMS amplitude of velocity and acceleration in the specimen are found as follows.

$$v_{rms} = \frac{k}{\rho\omega}\tau_{rms},$$
$$a_{rms} = \omega v_{rms} = \frac{k}{\rho}\tau_{rms} \quad \cdots\cdots\cdots\cdots (20)$$

where k is the wave number of the loading. From above relationship, the coefficient l in Eq. (14) is found to be 1/k, therefore,

$$A_c = \frac{k\kappa\sigma_{v0}'}{\rho}\tan\phi_c \quad \cdots\cdots\cdots\cdots (21)$$

where the initial effective confining stress σ_{mo}' in Eq. (14) is replaced with the initial effective vertical stress using a coefficient

$$\kappa = \frac{\sigma_{m0}'}{\sigma_{v0}'} = \frac{1+2K_0}{3} \quad \cdots\cdots\cdots\cdots (22)$$

which is related to the lateral stress coefficient K_0.

We derived the analytical form of the energy loss coefficient of soil in Eqs (10) and (11), by assuming that the internal friction of soil is idealized by the motion of a mass on a rough boundary. We will calculate the damping coefficient of our model for one dimensional sinusoidal loading. The damping coefficient h is defined as the ratio between the strain energy Es and energy lost during one cycle of loading ΔD:

$$h = \frac{1}{4\pi}\frac{\Delta D}{E_s} \quad \cdots\cdots\cdots\cdots (23)$$

where the strain energy is defined by using the amplitude of the shear strain γ_d:

$$E_s = \frac{1}{2}G\gamma_d^2 \quad \cdots\cdots\cdots\cdots (24)$$

By using stress amplitude in place of the strain amplitude and from Eq. (19), the strain energy Es in Eq. (23) is expressed by the mean kinematic energy:

$$E_s = \frac{\tau_d^2}{2G} = 2\bar{K} \quad \cdots\cdots\cdots\cdots (25)$$

The duration s_0 of one cycle of sinusoidal loading with angular frequency ω_v is $2\pi/\omega_v$. Therefore, the number of cycles of the energy wave defined in Eq. (13) is 2. Substitute this value into Eq. (10) and by denoting the energy lost during one cycle of sinusoidal loading by ΔD, the damping coefficient is found to be related to the mechanical loss coefficient of our model:

$$h = \frac{f}{2\pi} \quad \cdots\cdots\cdots\cdots (26)$$

Substituting $\alpha_v=1$ into Eq. (10), we find

$$f = \exp\left(-\frac{\kappa^2\tan^2\phi_c}{R_l^2}\right) \quad \cdots\cdots\cdots\cdots (27)$$

where

$$R_l = \frac{\tau_d}{\sigma_{v0}'} \quad \cdots\cdots (28)$$

stands for the stress ratio. **Fig.2** illustrates the damping coefficient of our model for ϕ_c=15 degrees and K_0=0.5, i.e. κ=2/3.

From Eqs. (15), (25) and (27), the energy stored in the pore-water after N cycles of sinusoidal loading is evaluated:

$$\Delta E_{ps} = \frac{\eta}{G}\tau_d{}^2 N \exp\left(- \frac{\kappa^2 \tan^2 \phi_c}{R_l^2} \right) \quad \cdots\cdots (29)$$

In the standard practice, the number N of cycles that are required to bring the specimen to yield 5% or 10% of the double amplitude of axial strain, is measured, keeping the stress ratio R_l as a specified value. We assume that the large strain corresponds to the pore-water pressure increment of almost equal to the initial effective vertical stress. Substituting $\Delta p = \sigma_{v0}'$ into Eq. (4), the increment of the strain energy in the pore-water is evaluated

$$\Delta E_{ps} = \frac{1}{2} n_f (1+2\beta) C \sigma_{v0}'^2 \quad \cdots\cdots (30)$$

where $\beta = p_0/\sigma_{v0}'$ is the initial pore-pressure ratio. From Eqs. (29) and (30), the R_l vs. N curve of cyclic shear test is analytically obtained in the normalized form,

$$\varepsilon^2 = R_l^2 N \exp\left(- \left(\frac{\kappa \tan \phi_c}{R_l} \right)^2 \right) \quad \cdots\cdots (31)$$

where

$$\varepsilon^2 = \frac{\Delta E_{ps}}{\left(\eta \sigma_{v0}'^2 / G\right)} = \frac{n_f}{2\eta}(1+2\beta) C G \quad \cdots\cdots (32)$$

is the normalized energy stored in the pore-water.

It is interesting that the effect of the frequency of loading on the analytical Rl vs. N curve could be inferred from Eq (20). Actually when we compute the mean energy in Eq. (19), it disappears to compensate for the wave number k and introduces a new material constant G into our formulation. Literally, the wave equation is contracted into our formula in the form of its constant $\omega/k = V_s$. The effect of the loading frequency has been extensively studied (e.g., Yasuda and Soga, 1984, Tatsuoka et al., 1986). At present, the experimental results show little bias for the loading frequency. And the analytical consequence of our model supports this fact.

Eqs. (31) and (32) show that, from the R_l vs. N curve, a pair of material quantities can be determined, namely the critical friction angle of dislocation ϕ_c and

$$C_e = \frac{C}{\eta} \quad \cdots\cdots (33)$$

which can be called the effective compressibility of the pore-water. To measure these quantities, it is convenient to transform the data point (N, Rl) into

$$X = \frac{1}{R_l^2}, \quad Y = \ln N R_l^2 \quad \cdots\cdots (34)$$

Since the analytical curve degenerates into a line on the X-Y plane;

$$Y = \left(\kappa \tan \phi_c\right)^2 X + \ln \varepsilon^2 \quad \cdots\cdots (35)$$

The following procedure results in the material constants of our model from the Rl vs. N curve obtained by the undrained cyclic loading test:

(1) Transform the test results (N, Rl) into (X, Y) by Eq. (34)

(2) Regress linearly Y against X, and calculate the estimate of the slope a and the Y-intercept b and compute the the critical angle of dislocation ϕ_c and normalized energy increment ε^2 by

$$\tan \phi_c = \frac{1}{\kappa}\sqrt{a}, \quad \varepsilon^2 = \exp(b) \quad \cdots\cdots (36)$$

(3) Find the mean shear modulus G from the strain amplitudes γ_{di} of the i'th cycle

$$G = \frac{\tau_d}{\gamma_d} = \frac{R_l \sigma_{v0}'}{\frac{1}{N}\sum_i^N \gamma_{di}} \quad \cdots\cdots (37)$$

and calculate the effective compressibility:

$$C_e = \frac{2\varepsilon^2}{n_f(1+2\beta)G} \quad \cdots\cdots (38)$$

Our analytical curve can be normalized by defining

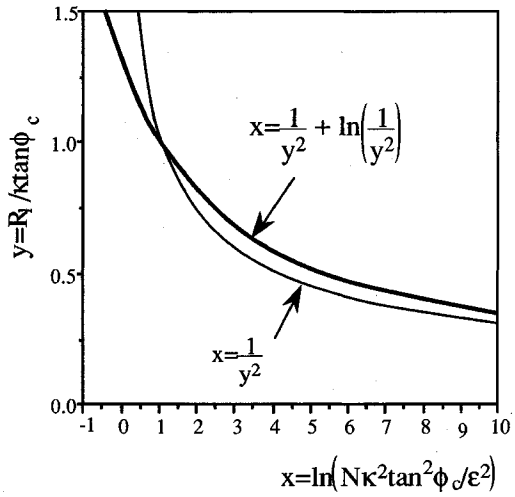

Fig. 3 Normalized Liquefaction Strength Curve

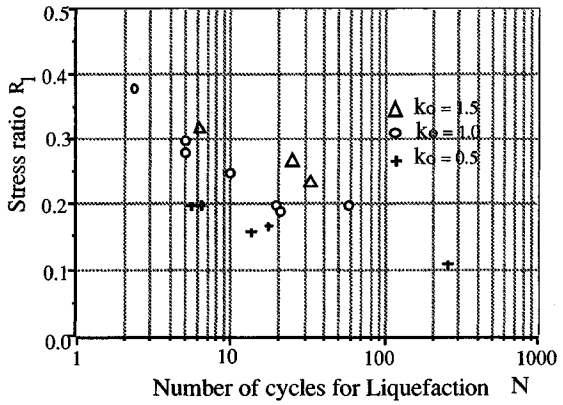

Fig. 4 Stress ratios of liquefaction for anisotropically consolidated sands

$$x = \ln N' = \ln\left(\frac{N\kappa^2\tan^2\phi_c}{\varepsilon^2}\right)$$

$$y = R_l' = \frac{R_l}{\kappa\tan\phi_c} \qquad \cdots\cdots\cdots\cdots (39)$$

into a simple curve on the (x,y) plane:

$$x = \frac{1}{y^2} + \ln\left(\frac{1}{y^2}\right) \cdots\cdots\cdots\cdots\cdots\cdots (40)$$

Clearly, this is a monotonically decreasing convex function, going through a fixed point of (1,1), shown in **Fig. 3**.

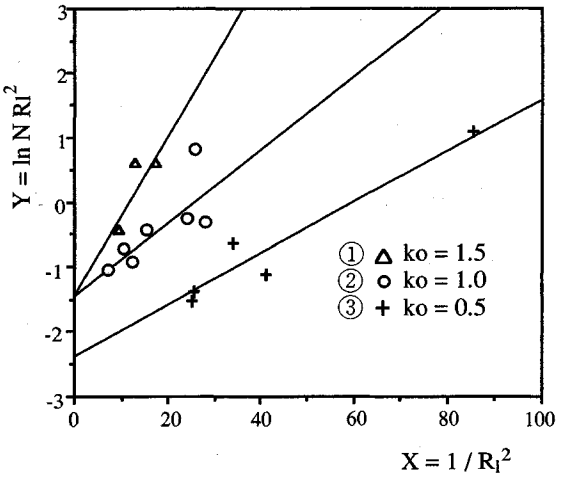

Fig. 5 Rl vs. Log N data transformed on to X-Y plane

Table 1 Liquefaction strength parameters of The Fuji River Sand

Lateral stress coeff. K_0	0.5	1.0	1.5
Normalized energy ε^2	8.72E-2	2.25E-1	2.26E-1
Compressibility C (Pa^{-1})	4.5E-10	4.5E-10	4.5E-10
Shear rigidity G(Pa)	1.355E+6	2.076E+6	2.796E+6
Dislocation angle ϕ_c(deg.)	16.8	13.7	15.1
Effective C. C_e (Pa^{-1})	9.965E-8	1.678E-7	1.252E-7
Energy absorption ratio η(%)	0.45	0.27	0.36

For a large N, the shape comes mostly from the first term, which, in the original equation, exponentially represents the form of the normal probability density function coming into our theory when the probability of the occurrence of the slip in a dislocation was computed. For a small N or a large stress ratio, the shape is determined by the second term, which corresponds to the R_l^2 term in Eq. (31). This means that for a large stress ratio, the effect of loading can be evaluated by its energy without considering the threshold. This analytical curve appears similar to the actual one. The experimental data will show us the essence of the liquefaction mechanism in its curvature.

6. EVALUATION OF LIQUEFACTION STRENGTH PARAMETERS

Now we are ready to test the theory; let us apply it to the well-referred experiment by Ishihara et al. (1977) and see what figures it produces out of the actual data: **Fig. 4** illustrates the R_l vs. log N curve obtained from the undrained torsional cyclic shear test conducted

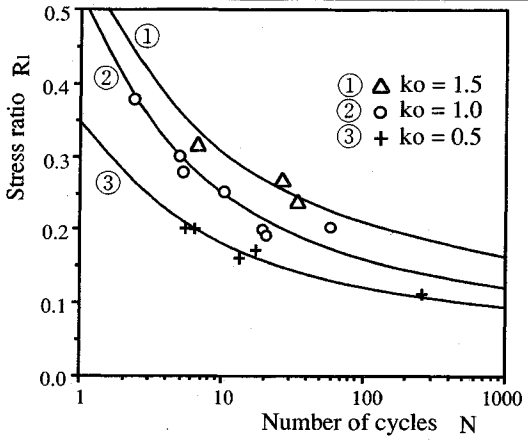

Fig. 6 Analytical liquefaction strength curves and experimental data

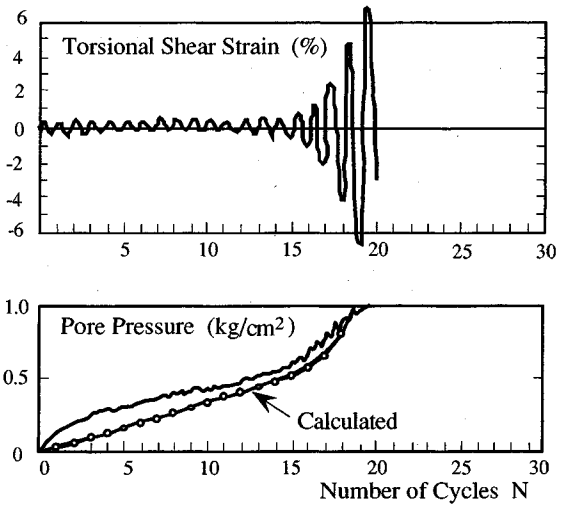

Fig. 7 Pore pressure and torsional shear strain record (Reproduced from Ishihara et. al., 1977)

under the initial effective vertical stress of 98 KN/m^2 with different K_0 values. The loading was sinusoidal with 1.0 Hz frequency. The initial pore-water pressure is 0 kgf/cm^2 in the gage scale, i.e. 1 atm=101.3 kN/m^3.

Fig. 5 shows how the data are located on the X-Y plane defined by Eq. (34); if our theory applies, the data should be on the line determined by Eq. (35), apparently true for this case, where the slope and the Y intercept are $(\kappa\tan\phi_c)^2$ and $\ln \varepsilon^2$, respectively. From Eq. (36), the normalized energy increase and critical angle of dislocation are computed and listed in **Table 1**. In **Fig. 6** the analytical R_l vs. log N curve with the above calculated constants are drawn.

The critical friction angles are calculated 16.8, 13.7, 15.1 degrees for the K_0 values of 0.5, 1.0, and 1.5 respectively. Their maximum deviation from the mean is 1.6 degree. The angles are practically unchanged for the different initial confining stresses; the normalized energy increase ε^2 appears to increase rapidly for K_0=0.5 to 1.0 but are almost unchanged for K_0=1.0 and 1.5. Our expression in Eq (32) states that ε^2 should change according to the shear rigidity G. Since ε^2 is determined from the Y-intercept of the X, Y plot, stress ratios of small N are necessary to estimate ε^2 precisely. For K_0=0.5 and 1.5, the data shifts towards a larger N when compared to K_0=1.0. This may have affected the deviation in ε^2 . In **Fig. 6**, the analytical curve for K_0=1.0 looks somewhat different from the other two.

The effective compressibility C_e can be evaluated from ε^2, provided the porosity n_f, initial pore-water pressure ratio β, and effective shear modulus G are known. Let us estimate G by Eq (37) from the amplitudes of cyclic shear stress τ_d and the shear strain record in **Fig. 7** (Ishihara et al., 1977). The shear stress amplitude τ_d is kept constant during the test, so, mean shear strain amplitude corresponds to the mean strain energy amplitude $\gamma_d\tau_d$. Therefore, for example, the mean strain amplitude of K_0=0.5, σ_{v0}'=98000 Pa, and R_l=0.155 is

$$\overline{\gamma}_d = \frac{1}{20}\left(0.45+0.3+\cdots+6.6\right) = 1.12\% \cdots (41)$$

and

$$G = \frac{\tau_d}{\gamma_d} = \frac{R_l\sigma_{v0}'}{\gamma_d} = 1.355\text{E+6 (Pa)} \cdots\cdots (42)$$

the rest of the pertinent material constants are n_f=0.421, ρ=1900 kg/m^3, ε^2=0.0872, β=1.034, and form Eq. (38)

$$C_e = \frac{C}{\eta} = 9.965\text{E-8 (Pa}^{-1}) \cdots\cdots\cdots\cdots (43)$$

Incidentally, the compressibility of the pore of loose sand is about C_p=1.8 x10^{-6} (Pa^{-1})(Ishihara, 1968), and that of the pure water at ordinary temperature is C=4.5x10^{-10}(Pa^{-1}). The computed value falls between the two, which can be deemed to bound the effective compressibility of the pore-water.

Table 1 lists the material constants obtained from the above computations, where both of the C_e and ϕ_c are practically unchanged. The constants are obtained

from the same sand and relative density (Dr=55%) but under different confining pressures. Therefore, this result can be considered to support our premise that the two constants represent the material characteristic of the soil.

Now our formulations are ready to predict the pore pressure increase due to a generic excitation. For example, they can compute the time history of the pore-water pressure during the torsional shear test; **Fig. 7** compares the calculated pore pressure and the recorded value for K_0=0.5 and R_l=0.155. The energy increase is computed by Eqs. (29) and (37), and pore-water pressure is calculated by Eq (4), using the η and ϕ_c obtained above. The calculated value is a good estimate of the actual mean pore pressure in this example.

7. LIQUEFACTION OF KAWAGISHI -CHO DURING 1964-NIIGATA EARTHQUAKE

Let us apply our method to the actual liquefaction observed during the 1964 Niigata earthquake. The procedure is as follows:

(1) Determine the effective compressibility C_e (Pa^{-1}) and critical friction angle ϕ_c (degree), for example by the undrained shear test. Evaluate the energy absorption ratio η from the effective compressibility C_e and the compressibility of the pore-water C in the specimen.

(2) Estimate intensity of the ground motion using strong motion parameters in Eqs. (9) through (13), namely, strong motion duration s_0 (sec), central frequency ω_v (rad/sec), RMS acceleration a_{rms} (m/sec^2), and bandwidth index α_v.

(3) Compute the critical acceleration of dislocation A_c (m/sec^2) by Eq (14) assuming a relationship between shear stress and acceleration in the ground.

(4) Calculate the strain energy increment in the pore-water ΔE_{ps} (J/m^3) by Eq (15) from the ground motion parameters and the critical acceleration.

(5) Evaluate the pore-water pressure generated during the ground motion by Eq (4) using the compressibility C of pore-water, porosity n_f, and the initial pore pressure p_0 (Pa).

In 1991, The JSSMFE conducted a cooperative analyses on the liquefaction observed in the ground beneath the Kawagishi-cho apartment during the 1964-Niigata earthquake. In **Table 2** is listed the soil properties used in the analyses. The resistance of the soil against liquefaction is specified by a pair of points on the R_l vs. logN chart. In **Fig.** 8, those points are plotted.

Table 2 Property of soil near the Kawagishi-chyo apartment Building

Depth H m	Density ρ kg/m^3	Initial rigidity G KP_a	Porosity n	Critical Dislocation Angle ϕ_c(degree)	Energy Absorption Ratio η (%)
Surface Soil ▽-2m	1800	21780			
Medium Sand -5m	1900	22990	0.475	11.9	9.57
Medium Sand -8m	1960	42750	0.469	11.9	4.71
Medium fine Sand -14m	1900	65030	0.466	13.5	2.67

Note: Compressibility of pore-water is assumed as 4.5E-10 Pa^{-1}.

Fig. 9 illustrates how these points are mapped on to the X-Y plane defined in Eq. (34). In this case, only a pair of points are specified, therefore they alone completely determine the regression lines. The critical friction angle ϕ_c and the energy absorption ratio of the pore-water η are calculated from the slope a and Y-intercept b of these lines and listed in **Table 2.** In **Fig. 8**, the analytical R_l vs. log N curve in Eq. (31) are drawn using these parameters along with the points specified.

These R_l and N values are not obtained by an actual experiment but are specified referring pertinent test results (Ishihara et al., 1981; Yoshimi et al., 1984).

Therefore, we assume the condition of the test necessary to determine the parameters as follows; the effective confining pressure and back pressure of pore-water are taken as in situ values; the effective shear modulus are assumed as 1/10 of the initial rigidity G_0 considering ordinary G/G_0 vs. γ curve where the mean shear strain amplitude becomes about 1%. When compared with the values obtained in Chapter 6 from the samples with Fuji River sand, the energy absorption ratios in **Table 2** is found to be about ten

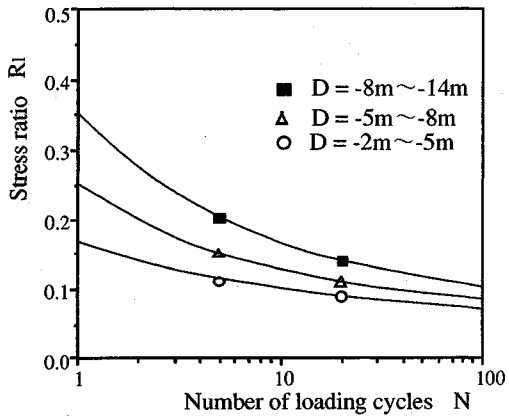

Fig. 8 Liquefaction strength curve of Kawagishi sand

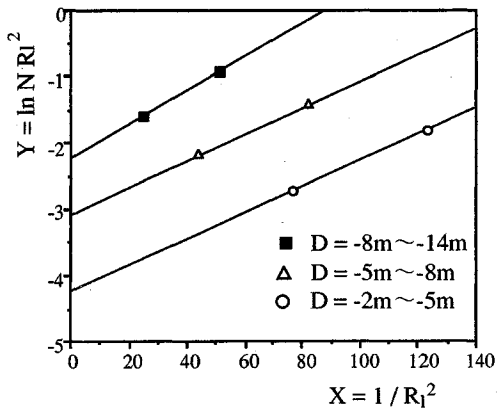

Fig. 9 X-Y plot of Kawagishi sand

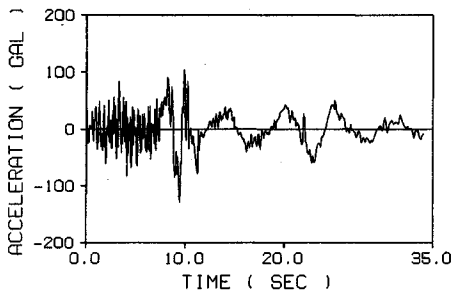

(a) NS Component

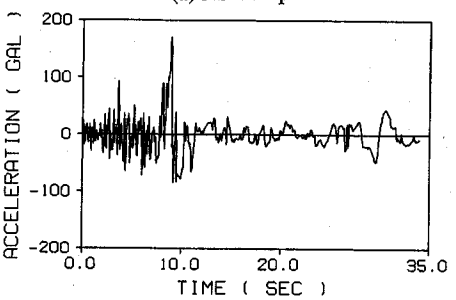

(b) EW component

Fig. 10 Accelerograms of Kawagishi-chyo

Table 3 Strong motion parameters of Kawagishi-chyo record (1964/06/16 13:01)

Component	Unit	NS	EW	Japan Mean	S.D.
Magnitude	JMA	7.5		6.71	0.90
Focal Depth	km	40		35.1	18.3
Epic. Dist.	km	59		86.3	18.28
Rec. Duration(T_0)	sec	34.02	33.92	56.58	35.72
Rec. Peak Acc.	m/s^2	1.319	1.619	1.423	0.815
Correct. Peak Acc.	m/s^2	1.289	1.709	1.765	1.014
RMS Acc. (a_{rms})	m/s^2	0.479	0.760	0.674	0.478
Str. Duration (s_0)	sec	11.76	4.18	11.88	12.39
Central Freq. (ω_a)	rad/s	15.78	14.37	29.13	11.28
Bandwidth I. (α_v)		0.120	0.170	0.410	0.152
RMS Vel. (v_{rms})	m/sec	0.253	0.313	0.079	0.074
Central Freq. (ω_v)	rad/s	1.894	2.42	12.17	7.31
No. of Cycles (N_v)		7.10	3.24	46.4	91.0
Total Kinematic Energy	J/m^3	431	300	217.1	442.3

Note: ρ=1900kg/m^3 is assumed for computing kinematic energy.

Table 4 Calculated excess pore-water pressure ratios and liquefaction time T_l

(a) Beneath the apartment building

Depth H (m)	σ_{v0}' (KPa)	$\Delta p/\sigma_{v0}'(T0)$	T_l (sec)
3.5	80	2.36	14.4
6.5	100	3.31	10.3
11.0	130	0.92	36.8

(b) Near the apartment building (Free surface)

Depth H (m)	σ_{v0}' (KPa)	$\Delta p/\sigma_{v0}'(T_0)$	T_l (sec)
3.5	50	11.45	3.0
6.5	75	6.74	5.0
11.0	125	1.08	31.4

Note: the values greater than unity indicate that the dislocation energy of the entire ground motion is larger than the value just necessary for liquefaction.

times larger, while the friction angles are similar. Actually, the liquefaction strength curves of the Fuji River sand in **Fig. 6** shift upward in comparison to those in **Fig. 8**. The number 3 curve in **Fig. 6** is similar to that for the depth -8m to -14m in **Fig. 8**. The energy absorption ratios of these two curves are 0.45 and 2.67, the latter is about 6 times larger than the former. This difference comes mostly from that in the estimates of the effective rigidity G and slightly from that in the initial pore-water pressure ratios β. From Eqs.(33) and (38), we find that the energy absorption ratios η increase proportionally with G for the same normalized energy ε^2 which is determined from the liquefaction strength curve.

The SMAC-A strong-motion seismograph has been installed in the basement of the No. 2 apartment of Kawagishi-cho. The accelerogram was processed by the NOAA for instrumental and digitizing error correction (1981). **Fig. 10** plots those time histories. 3 to 4 seconds after the triggering time, both components decrease the amplitude as well as the frequency. This appears to show the occurrence of liquefaction.

In **Table 3** are listed the pertinent parameters of the NS and EW components associated with the mean values of the 52 major Japanese strong motion records (Igarashi, 1989). The accelerograms are distinguished from the Japanese data set by the followings; they are of the type where a big earthquake is recorded not far from the epicenter; they have a large energy and wide variety of frequencies; α_v is small; v_{rms} is large. The kinematic energy density is more than twice as much as the Japanese mean. The ground is classified to be 3rd in the JSCE scale; the peak acceleration is not large, whereas the energy density is remarkably high.

The pertinent parameters in **Tables 2 and 3** are processed according to steps (1) through (5), where we assumed that the strain energy accumulation in the pore-water can be computed separately for NS and EW components and that the total energy increase can be computed by adding them:

$$\Delta E_{ps}=\left(\Delta E_{ps}\right)_{NS}+\left(\Delta E_{ps}\right)_{EW} \quad \cdots\cdots\cdots\cdots (44)$$

The excess pore-water pressure ratios $\Delta p/\sigma_{v0}'$ are computed for the initial effective vertical pressures presumed to be beneath the center of the apartment and the free surface nearby. We disregarded the physical upper bound of the excess pore pressure ratio of 1.0; the figures greater than unity can be interpreted to indicate that the soil is liquified in the early part of the excitation before its accumulated energy reaches the final value of the total kinematic energy. This corresponds to the report by Tokimatsu (1989); he concluded that the soil surrounding the apartment was probably liquified 6 seconds after the triggering time of the accelerogram, judging from the fact that the time history changed its dominant Period from about 0.5 sec to 5 sec at that time. Let us estimate the time of liquefaction T_l from the final excess pore pressure ratio $\Delta p/\sigma_{v0}'(T_0)$ calculated in **Table 4.**, by assuming that the pore pressure accumulates stationarily:

$$T_l=\frac{T_0}{\Delta p/\sigma_{v0}'(T_0)} \quad \cdots\cdots\cdots\cdots\cdots\cdots (45)$$

in which T_0=34 secs stands for the record duration. In **Table 4**, the estimates of the time of complete liquefaction for each layer. They are about 14.4 secs and 10.3 secs for D=-3.5m and -6.5m, beneath the apartment, about 3.0 secs and 5.0 secs, for the free surface, respectively. The Tokimatsu's estimation of 6 secs falls between these values.

The excess pore pressure ratios for the depth of 11.0m are computed about 0.92 and 1.08 in **Table 4** (a) and (b). These figures imply that the liquefaction occurred down to this depth. This sounds realistic judging from the field reports and on the famous photograph where an apartment building turned over completely (Tokimatsu,1989). The dislocation energy concept produced a realistic result in this example.

8. CONCLUSIONS

A theory of liquefaction is derived on the premises that the energy accumulated in the pore-water is proportional to the energy dissipated through plastic deformation of soil with a factor called energy absorption ratio η and that the internal friction of soil is idealized by the sliding block model. The energy stored in the pore-water is called dislocation energy. Out of this study, the following can be concluded:

1) For some type of soil, the strength of soil against liquefaction can be represented by a pair of material quantities, namely effective compressibility of pore-water C_e and the critical friction angle of dislocation ϕ_c. Judging from the illustrations, sand with a medium relative density falls within this category.

2) The liquefaction observed near the Kawagishi-cho apartment during the 1964-Niigata earthquake was explained clearly by the dislocation energy concept, using parameters computed from the soil conditions specified by JSSFME and the accelerograms recorded in the basement of the apartment.

3) The theory based on the dislocation energy concept as well as the energy-related parameters of ground motions are proved effective in predicting liquefaction.

9. ACKNOWLEDGMENTS

The author expresses his hearty gratitude to Professor Motohiko Hakuno for his invaluable suggestions and encouragement, without which this study would not have been possible. He is grateful to Messrs. Yoshishige Ito and Katsumi Kamemura of Taisei Corporation for the invariant support. Last but not

least, he is indebted to Dr. Jiro Kuwano and Mrs. Reiko Kuwano in reviewing manuscripts.

REFERENCES

1) Biot, M. A. : Theory of Propagation of Elastic Waves in a Fluid-Saturated Porous Solid. I. Low-Frequency Range, The Journal of the Acoustical Society of America, pp. 168-178, 1956.

2) Ishihara,K. : Approximate forms of wave equations for water-saturated porous materials and related dynamic modulus, Soils and Foundations Vol.x, No.4, pp. 11-38, 1970.

3) Myers, H.P.: Introductory Solid State Physics, Taylor & Francis, London, 1990.

4) Suzuki, H. :Introduction to Dislocation Theory (in Japanese), Agune, Japan, 1967.

5) Cocks and Ponter : Constitutive equations for the plastic deformation of solids. I. Isotropic material, Europian Journal of Mechanics, A/solids, Vol. 10 #3, pp. 243-264, 1991.

6) Titchener, A.L. and Beven M.B.: The stored energy of cold work, Prog. Met. Phys, #7, pp.247-338, 1958.

7) Igarashi, S. and Hakuno, M. : The Response of Mass-on-Rough-Plane Model due to Earthquakes, Proc. of JSCE, Vol 4, No. 1, pp. 223-233, 1987.

8) Vanmarcke, E. H., Lai, S. P. : Strong-Motion duration and RMS amplitude of Earthquake Records, Bull. of the Seismological Society of America, Vol 70, No. 4, pp. 1293-1307, , 1980.

9) Toki, S., Tatsuoka, F., Miura, S., Yoshimi, Y.,Yasuda , Y.and Makihara,Y. : Cyclic Undrained Triaxial Strength of Sand by a Cooperative Test Program, Soils and Foundations Vol.26, No.3, pp. 117-128, 1986.

10) Yasuda,S., Soga, M. : Effect of Loading Frequency on Cyclic Shear Test, Proc. of 19th Japanese Soil Mechanics and Foundation Engineering Symposium, pp. 99-116 (in Japanese), 1984.

11) Tatsuoka, F., Toki, S., Miura, S., Kato, H., Okamoto, M., Yamada, S., Yasuda, S. and Tanizawa, F. : Some Factors Affecting Cyclic Undrained Triaxial Strength of Sand, Soils and Foundations Vol 26, No.3, pp. 451-467, 1986.

12) Ishihara, K. : Propagation of Compressional Waves in a Saturated Soil, Proc. of the Intl. Symposium of Wave Propagation and Dynamic Properties of Earth Materials, Univ. of New Mexico Press, pp. 451-467, 1968.

13) Ishihara, K., Iwamoto,S., Yasuda, S., Takatsu, H. : Liquefaction of Anisotropically Consolidated Sand, Proc. 9th ICSMFE, Vol.2, pp. 261-264, 1977.

14)Japan Society of Soil Mechanics and Foundation Engineering : Proc. of Symposium on the Counter Measures against Liquefaction, in Japanese, 1991.

15)Japan Society of Soil Mechanics and Foundation Engineering : Proc. of Symposium on the Behavior of Soil and Structure during Earthquakes, in Japanese, 1989.

16)National Oceanic and Atmospheric Administration: Strong Motion Data from Japanese Earthquakes, 1981.

17) Ishihara, K. and Koga, Y. : Case studies of liquefaction in the 1964 Nigata earthquake, Soils and foundations Vol.21, No.3, pp. 35-52, 1981.

18) Igarashi, S. : Analysis and Prediction of Earthquake-Induced Permanent Displacement in Gravity-type and Soil Structures, Doctoral Dissertation, Univ. of Tokyo,1989.

(19) Tatsuoka, F., Ochi, K., Fujii, S. and Okamoto, M.: Cyclic Undrained Triaxial and Torsional Shear Strength of Sands for Different Sample Preparation Methods, Soils and Foundations Vol.26, No.3, pp. 23-41, 1986.

(Received November 9, 1991)

液状化の転位エネルギー

五十嵐　俊一

土の塑性変形と，間隙水圧の上昇過程のエネルギー的考察から，液状化現象を説明する理論を導く．土の塑性変形は，土粒子骨格の局所的に滑り易い構造（転位）に局所化されていると仮定し，限界転位角と呼ぶ摩擦角で塑性変形のエネルギー損失（減衰）を表す．これと，間隙水圧に蓄えられる歪みエネルギーを関係づけるものとして，エネルギー吸収率と呼ぶ物性値を定義する．これらの物性値は，液状化強度曲線から決定できることをしめす．新潟地震の川岸町の液状化事例に適用し，この理論の有効性を確かめる．